Microelectronic Engineering 85 (2008) 1866–1871

Contents lists available at ScienceDirect

Microelectronic Engineering

journal homepage: www.elsevier.com/locate/mee

Study on the frequency dependence of electrical and dielectric characteristics of Au/SnO_2/n-Si (MIS) structures

A. Tataroğlu *, Ş. Altındal

Physics Department, Faculty of Arts and Sciences, Gazi University, 06500 Teknikokullar, Ankara, Turkey

ARTICLE INFO

Article history:
Received 25 January 2008
Received in revised form 30 April 2008
Accepted 26 May 2008
Available online 3 June 2008

Keywords:
MIS structure
Electrical characteristics
Dielectric characteristics
Ac conductivity
Ac resistivity
Electric modulus

ABSTRACT

In this paper, we present a detailed investigation of the electrical and dielectric properties of the Au/SnO_2/n-Si (MIS) structures. The capacitance–voltage (C–V) and conductance–voltage (G/ω–V) characteristics have been measured in the frequency range of 1 kHz–1 MHz at room temperature. Calculation of the dielectric constant (ϵ'), dielectric loss (ϵ''), loss tangent ($\tan\delta$), ac electrical conductivity (σ_{ac}), ac resistivity (ρ_{ac}) and the electric modulus are given in the studied frequency ranges. Experimental results show that the values of dielectric parameters are a strong function of frequency. The decrease of ϵ' and ϵ'' with increasing frequency were observed. In addition the increase of σ_{ac} with increasing frequency is founded. Also, electric modulus formalism has been analyzed to obtain the experimental dielectric data. The interfacial polarization can be more easily occurred at the lower frequency and/or with the number of interface state density between SnO_2/Si interface, consequently, contribute to the improvement of dielectric properties of MIS structure.

1. Introduction

Tin oxide films (SnO_2) have very interesting physical properties [1–3] such as high electrical conductivity coupled with fairly large optical transmission in the visible region, low resistivity, a wide band gap high transmittance to visible radiation and reflect infrared. Also, SnO_2 is material used in numerous technological applications, such as transparent electrodes, gas detectors, far-infrared detectors, high efficiency solar cells [4,5] and lithium ion batteries [5,6]. SnO and SnO_2 oxides of tin are two stable oxide films exist in tetragonal crystallographic form. However in thin film form, depending on prepared temperature and deposition method its structure can be polycrystalline or amorphous [7]. The SnO_2 thin films are n-type semiconductor with direct optical band-gap of ~3.6–4.3 eV [7,8] and SnO is a metastable material at ambient condition when heated up at certain temperature it changes to more stable SnO_2 thin structure. There are several methods to prepare SnO_2 film such as electron beam evaporation, thermal evaporation of oxide powders, chemical vapor deposition (CVD), magnetron sputtering, spray deposition, sol–gel, etc.

Among them, the spray deposition process present an easy way to integrate SnO_2 devices into the Si technology, since it offers the possibility of good control of the deposition parameters, low processing temperatures and low production costs.

The metal–insulator–semiconductor (MIS) structures consist of semiconductor substrate that is covered by an insulator layer on which a metal electrode is deposited. Therefore, there structures constitute a kind of capacitor, which stores the electronic charges by virtue of dielectric property of insulator layers. The electrical characteristics of these structures are influenced by various non-idealities such as the interface states (N_{ss}), series resistance (R_s) and interfacial insulator layer [9–11]. Especially the performance and reliability of these structures are depending on the formation of insulator layer between metal and semiconductor interface and series resistance of devices. Also, the change in temperature has important effects on determination of structure parameters [12–14].

In general, there are several possible sources of error, which cause deviations from the ideal behavior. So, in calculations such as electrical and dielectric properties that includes the effects of interfacial insulator layer between metal and semiconductor; interface state density, series resistance and formation of barrier height must be taken into account. Nevertheless satisfactory understanding in all details has still not been achieved. Especially, the formation and characterization of SnO_2 insulator layers on Si substrate still remains a basic problem. It is well known that the high frequency electrical properties of MIS or MOS devices at in the accumulation region describe basically the dielectric properties of the bulk oxide. Therefore, the real dielectric parameters of these devices were extracted from the strong accumulation capacitance and conductance. Thus, the effect of interface states (N_{ss}) can be

* Corresponding author. Tel.: +90 312 202 1268; fax: +90 312 212 2279.
E-mail address: ademt@gazi.edu.tr (A. Tataroğlu).

0167-9317/$ - see front matter © 2008 Elsevier B.V. All rights reserved.
doi:10.1016/j.mee.2008.05.025

minimized at sufficiently high frequency C–V and G/ω–V measurements.

At high frequencies ω (such the carrier life time τ is much larger than $1/\omega$) the charges at the interface states cannot follow an ac signal. In contrary, at low frequencies the charges can easily follow an ac signal and they are capable of increase with decreasing frequency. Therefore, the frequency dependent electrical and dielectric characteristics are very important according to accuracy and reliability of result [15–19]. When SnO_2 compared to SiO_2, SnO_2 has actually a much more favorable position with its physical properties. Its main advantages are low density of interface states and high dielectric properties. Also, the formation of SnO_2 on Si by traditional ways of oxidation or deposition cannot completely passivate the active dangling bonds at the Si surface. Therefore, in this study, thin SnO_2 films on the n-Si substrate were prepared by a spraying deposition method.

This paper presents a detailed study on the electrical and dielectric properties in the frequency range of 1 kHz–1 MHz at room temperature for Au/SnO_2/n-Si (MIS) structure. To determining the dielectric constant (ϵ'), dielectric loss (ϵ''), loss tangent ($\tan\delta$), the ac electrical conductivity (σ_{ac}), ac resistivity (ρ_{ac}) and the electric modulus of MIS structure was used the admittance technique [15,16]. Also, it is well know, both electrical and dielectric properties of MIS structure significantly changes with frequency.

2. Experimental detail

The metal–insulator–semiconductor (Au/SnO_2/n-Si) structures used in this work were fabricated using n-type (P-doped) single crystals silicon wafer with ⟨1 1 1⟩ surface orientation, 280 μm thick, 2″ diameter and 4.45 Ω cm resistivity. The Si wafer was decreased for 5 min in boiling trichloroethylene, acetone and ethanol consecutively and then etched in: first H_2SO_4, H_2O_2 and 20% HF solution, then 6HNO_3: 1HF: 35H_2O and 20% HF solution. After each cleaning step, the wafer was rinsed thoroughly in de-ionized water of 18 MΩ cm resistivity. To remove any native thin oxide layer on the Si surface, the samples were dipped in HF:H_2O (1:10) about 20 s and finally the wafers were rinsed by ultrasonic bath in de-ionized water for a prolonged time. After surface cleaning, high purity Au metal (99.999%) with a thickness of 2500 Å was thermally evaporated from the tungsten filament onto the whole back surface of the wafer in liquid nitrogen trapped oil-free ultra-high vacuum system in the pressure of 1×10^{-6} Torr. To form low-resistivity ohmic contacts, Au back contacts were formed by thermal annealing at about 500 °C for 5 min in flowing dry nitrogen (N_2) in a quartz tube furnace. Immediately after ohmic contact, a thin layer of SnO_2 was grown on the Si substrate by spraying a solution consisting of 32.21 wt% of ethyl alcohol (C_2H_5OH), 40.35 wt% of de-ionized water (H_2O) and 27.44 wt% of stannic chloride ($SnCl_4 \times 5H_2O$), which was maintained at a constant temperature of 400 °C. The temperature of the substrates was monitored by chromel–alumel thermocouple fixed on top surface of the substrate. The variation of the substrate temperature during spray was maintained within ±2 °C with the help of a temperature controller. The rate of spraying was kept at about 30 cm^3/min by controlling the carrier gas flow-meter. N_2 was used as the carrier gas. SnO_2 dots were 4 mm in diameter. After spraying process, circular dots of 1 mm in diameter and 2500 Å thick Au rectifying contacts were deposited onto the SnO_2 surface of the wafer through a metal shadow mask in liquid nitrogen trapped oil-free ultra-high vacuum system in the pressure of 1×10^{-6} Torr. Both the thickness of metal layer and deposition rates were monitored with the help of a digital quartz crystal thickness monitor. The deposition rates were about 1–3 Å/s. The wafer was mounted on a copper holder with the help of silver paste and the electrical contacts were made to the upper electrodes by the use of tiny silver coated wires with silver paste. The interfacial oxide layer thickness was estimated to be about 46 Å from measurement of the oxide capacitance in the strong accumulation region for MIS structure.

The capacitance–voltage (C–V) and conductance–voltage (G/ω–V) measurements were carried out in the frequency range of 1 kHz–1 MHz at room temperature using a HP 4192A LF impedance analyzer (5 Hz–13 MHz) and a test signal 50 mV_{rms}. In addition, all measurements were carried out with the help of a microcomputer through an IEEE-488 ac/dc converter card.

3. Results and discussion

3.1. Electrical properties

The conductance technique [9,10] is based on the conductance losses resulting from the exchange of majority carriers at the interface and majority carrier band of the semiconductor when a small ac signal is applied to the metal–insulator–semiconductor (MIS) structure. The applied ac signal causes the Fermi level to oscillate about the mean positions governed by the dc bias, when the MIS structure is in the depletion region.

Fig. 1a and b show the C–V and G/ω–V characteristics of the structure at various frequencies. It can be seen from Fig. 1a that at low frequencies, the values of capacitance are shown to increase. The frequency dependence of the capacitance can also arise due to the presence of deep lying impurities in the depletion region of semiconductor. Deep impurities are the energy levels of intrinsic lattice defects or impurity atoms that have energy near the center of the band-gap. Presence of deep traps in the depletion region of the Schottky barrier makes the junction capacitance a complicated function of the bias voltage and the measuring frequency. The higher values of capacitance at low frequencies are due to excess capacitance resulting from the interface states in equilibrium with the n-Si that can follow the ac signal. Also, it is observed that the low-frequency capacitance increases with the applied bias while the high frequency capacitance remains almost constant. This observation may be attributed to the capacitive response of interface states to the measurement. At high frequencies ω (such the carrier life time τ is much larger than $1/\omega$) the charges at the interface states cannot follow the ac signal. This makes the contribution of interface state capacitance to the total capacitance negligibly small [20]. In general, at sufficiently high frequencies ($f \geqslant 500$ kHz) the interface states do not contribute to the capacitance [20–22]. Furthermore, as seen in Fig. 1b, the values of conductance give a peak at low frequencies about 3 V. Such behavior of the G/ω peaks is attributed to particular distribution of surface states between Si/SnO_2 interface.

3.2. Dielectric properties

The frequency dependence of dielectric constant (ϵ'), dielectric loss (ϵ''), loss tangent ($\tan\delta$), ac electrical conductivity (σ_{ac}), ac resistivity (ρ_{ac}) and electric modulus (M') are studied for MIS structure. At room temperature, the values of the dielectric properties measured as a function of frequency in the 1 kHz–1 MHz range.

The complex permittivity can be defined in the following complex form [23,24],

$$\epsilon^*(\omega) = \epsilon'\omega - i\epsilon''\omega \quad (1)$$

where ϵ' and ϵ'' are the real and the imaginary parts of complex permittivity, and i is the imaginary root of −1. The complex permittivity formalism has been employed to describe the electrical and dielectric properties. In the ε^* formalism, in the case of admittance measurements, the following relation holds:

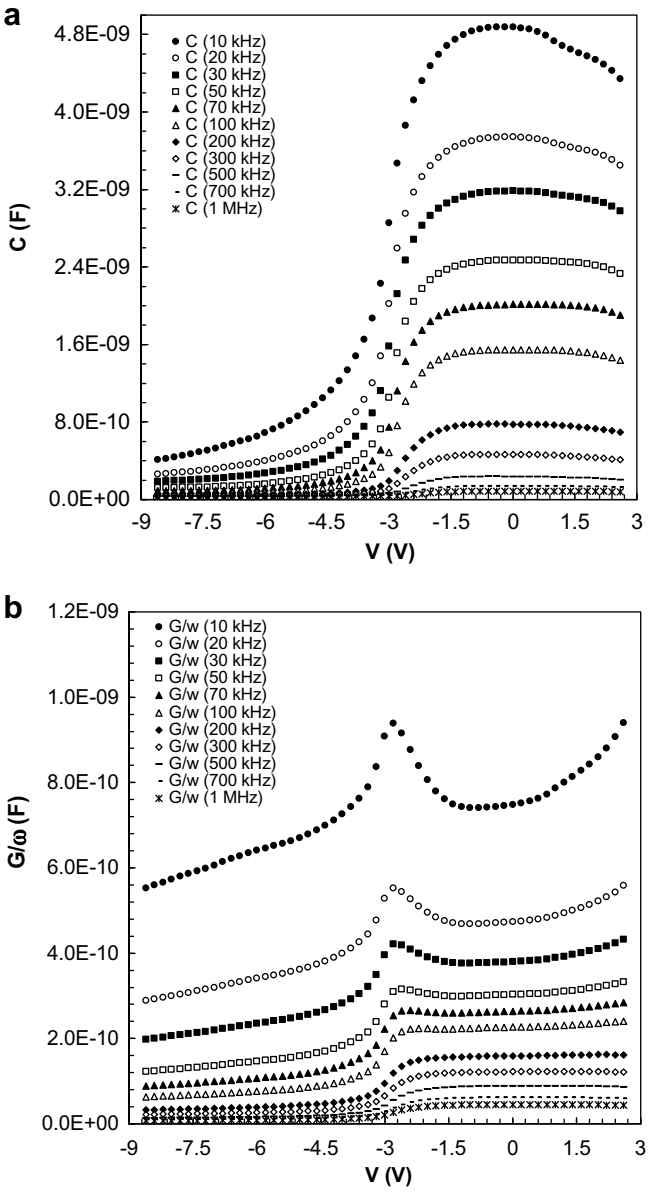

Fig. 1. The variations of the (a) C–V and (b) G/ω–V characteristics of Au/SnO_2/n-Si (MIS) structure measured for various frequencies at room temperature.

$$\varepsilon^* = \frac{Y^*}{j\omega C_0} = \frac{C}{C_0} - i\frac{G}{\omega C_0} \tag{2}$$

where Y^*, C and G are the measured admittance, capacitance and conductance of the dielectric and $\omega\ \imath\sigma$ the angular frequency ($\omega = 2\pi f$) of the applied electric field [25].

As it turns out the effect of conductivity can be highly suppressed when the data are presented in the modulus representation. The electric modulus approach began when the reciprocal complex permittivity was discussed as an electrical analogue to the mechanical shear modulus [25]. From the physical point of view, the electrical modulus corresponds to the relaxation of the electric field in the material when the electric displacement remains constant. Therefore, the modulus represents the real dielectric relaxation process [26,27]. The complex modulus $M^*(\omega)$ was introduced to describe the dielectric response of non-conducting materials. This formalism has been applied also to materials with non-zero conductivity. The starting point for further consideration is the definition of the dielectric modulus [25,28].

$$M^*(\omega) = \frac{1}{\varepsilon^*} = M'(\omega) + iM''(\omega) \tag{3}$$

$$M'(\omega) = \frac{\varepsilon'(\omega)}{\varepsilon'(\omega)^2 + \varepsilon''(\omega)^2} \quad \text{and} \quad M''(\omega) = \frac{\varepsilon''(\omega)}{\varepsilon'(\omega)^2 + \varepsilon''(\omega)^2} \tag{4}$$

where M' and M are the real and the imaginary of complex modulus. Based on Eq. (4) we have changed the form of presentation of the dielectric data from $\varepsilon'(\omega)$ and $\varepsilon''(\omega)$ to $M'(\omega)$ and $M(\omega)$.

The real part of the complex permittivity, the dielectric constant (ϵ'), at the various frequencies is calculated using the measured capacitance values at the strong accumulation region from the relation [29–31],

$$\varepsilon'(\omega) = \frac{C}{C_0} \tag{5}$$

where C_0 is capacitance of an empty capacitor. $C_0 = \varepsilon_0(A/d)$; where A is the rectifier contact area in cm^{-2}, d is the interfacial insulator layer thickness and ε_0 is the permittivity of free space charge ($\varepsilon_0 = 8.85 \times 10^{-14}$ F/cm). In the strong accumulation region, the maximal capacitance of MIS structure corresponds to the insulator capacitance (C_{0x}) ($C_{ac} = C_{0x} = \varepsilon'\varepsilon_0 A/d$); where ϵ' is the dielectric constant of interfacial insulator layer ($\epsilon' = \varepsilon_i = 7\varepsilon_0$).

The imaginary part of the complex permittivity, the dielectric loss (ϵ''), at the various frequencies is calculated using the measured conductance values from the relation,

$$\varepsilon''(\omega) = \frac{G}{\omega C_0} \tag{6}$$

The dissipation factor or loss tangent ($\tan\delta$) can be expressed as follows [23,24,29–31],

$$\tan\ \delta = \frac{\varepsilon''(\omega)}{\varepsilon'(\omega)} \tag{7}$$

The ac conductivity of all samples has been calculated from the dielectric losses according to the relation

$$\sigma^* = i\epsilon_0\omega\epsilon^*(\omega) = i\epsilon_0\omega(\epsilon' - i\epsilon'') = \epsilon_0\omega\epsilon'' + i\epsilon_0\omega\epsilon' \tag{8}$$

The real part of $\sigma^*(\omega)$ is given by

$$\sigma_{ac} = \omega C \tan\ \delta(d/A) = \varepsilon_0\omega\varepsilon'' \tag{9}$$

The frequency dependencies of the ϵ', ϵ and $\tan\delta$ of Al/SnO_2/p-Si (MIS) structure are presented in Fig. 2a–c, respectively. From the measured values of capacitance and conductance, the values of the ϵ', ϵ'' and $\tan\delta$ were found to be a strong function of frequency. As can be seen from these figures, ϵ' and ϵ'' decrease with an increase in frequency. This is the normal behavior of a dielectric material. In principle, at low frequencies and temperature, all the four types of polarization processes, i.e., the electronic, ionic, dipolar, and interfacial or surface polarization contribute to the values of ϵ' and ϵ''. With increasing frequency, the contributions of the interfacial, dipolar or the ionic polarization become ineffective by leaving behind only the electronic part. Furthermore, the decrease in ϵ' and ϵ with an increase in frequency is explained by the fact that as the frequency is raised, the interfacial dipoles have less time to orient themselves in the direction of the alternating field [32–37]. The ϵ' and ϵ'' have a values of 6.95, 3.01 at 1 kHz. This result shows that the strong low-frequency dispersion that characterizes the frequency dependence for the ϵ' and ϵ'' of MIS structure (in Fig. 2a and b) has not been clearly understood. But in general, four possible mechanisms; electrode interface, ac conductivity, dipole-orientation and charge carriers may be contributed to be low-frequency dielectric behavior of MIS structure [33,35–38].

Especially, in the high frequency range, the values of ϵ' become closer to the values of ϵ. This behavior of ϵ' and ϵ'' may be due to the interface states cannot follow the ac signal at high frequency. Because the carrier lifetime of interface trapped charges (τ) are

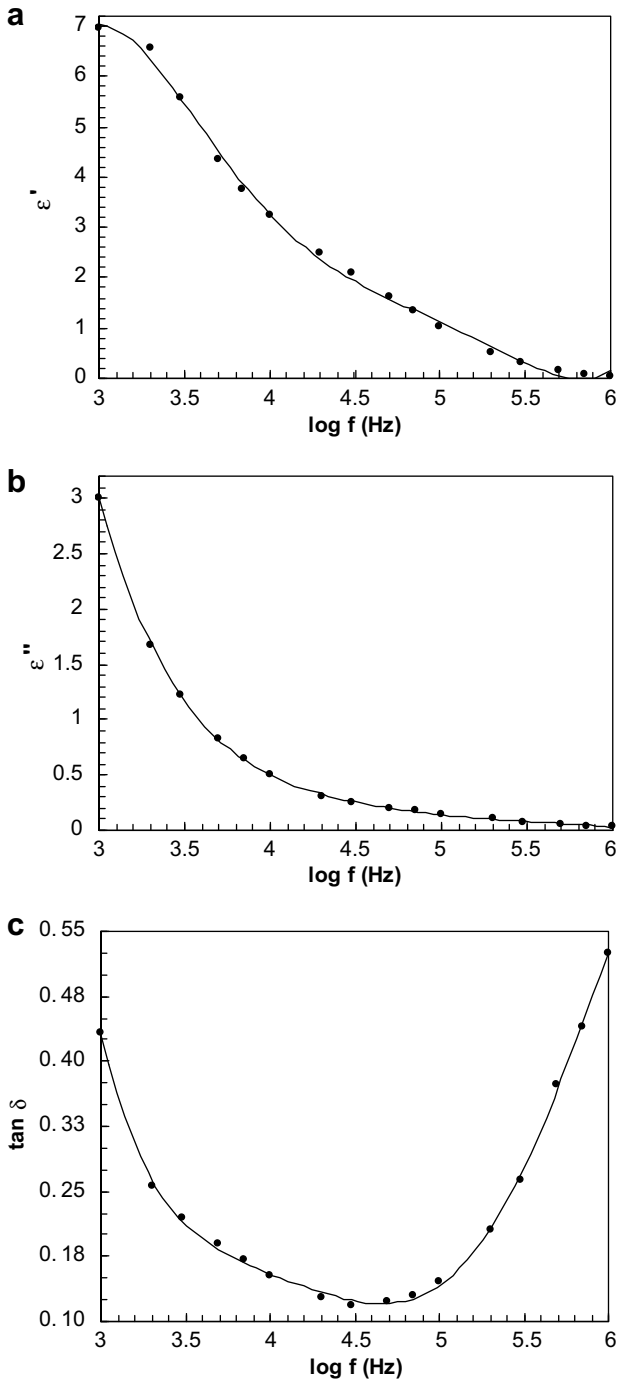

Fig. 2. Frequency dependence of the (a) ϵ', (b) ϵ'' and (c) $\tan\delta$ at room temperature for Au/SnO_2/n-Si (MIS) structure.

much larger than $1/\omega$ at very high frequency (ω). Such this behavior was observed by several authors [31,34,39–41].

Fig. 2c shows the variation of the loss tangent ($\tan\delta$) with frequency at room temperature. If the electric polarization in a dielectric is unable to follow the varying electric field, dielectric loss occurs. An applied field will alter this energy difference by producing a net polarization, which lags behind the applied field because the tunneling transition rates are finite. This part of the polarization, which is not in phase with the applied field, is termed as dielectric loss [42]. As shown in Fig. 2c, in the frequency range from 1 to 50 kHz the $\tan\delta$ decreases with increasing frequency, but approximately in the frequency range from 50 kHz to 1 MHz the

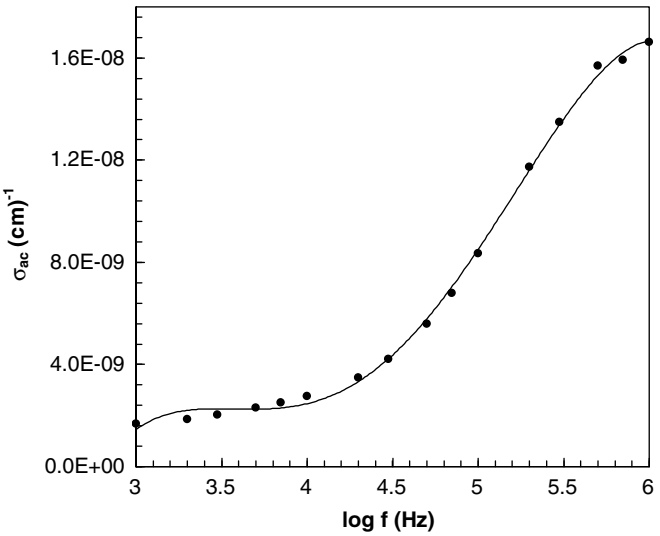

Fig. 3. Frequency dependence of ac electrical conductivity (σ_{ac}) for MIS structure at room temperature.

$\tan\delta$ increases with increasing frequency. It is clear that $\tan\delta$ is in close relation with the conductivity. The increase of the conductivity σ is accompanied by an increase of the eddy current.

Fig. 3 illustrates the dependence of the ac electrical conductivity (σ_{ac}) on the frequency. Fig. 3 depicts the variation of the ac conductivity σ_{ac} with frequency (in the frequency range 1 kHz–1 MHz) at room temperature for MIS structure.

It is noticed that the σ_{ac} decreases with decreasing frequency. This behavior is typical for this structure and can be ascribed to the space charge polarization. As the frequency decreases, more and more charge accumulation occurs at the insulator–semiconductor interface, which leads to a drop in the conductivity at low frequencies. Similar behavior was observed in the literature [32–34,38,43,44].

Fig. 4 shows the variation of ac resistivity (ρ_{ac}) with log frequency at room temperature. All the samples show a decrease in ρ_{ac} with increase in frequency from 1 kHz to 1 MHz. The increase in frequency of the applied field enhances the hopping of charge carriers resulting in increase of conductivity and decrease of resistivity. At higher frequencies ac resistivity decreases and remains constant because of the fact that hopping frequency can no longer follow the frequency of the applied external field leading to lower values of ac resistivity [45].

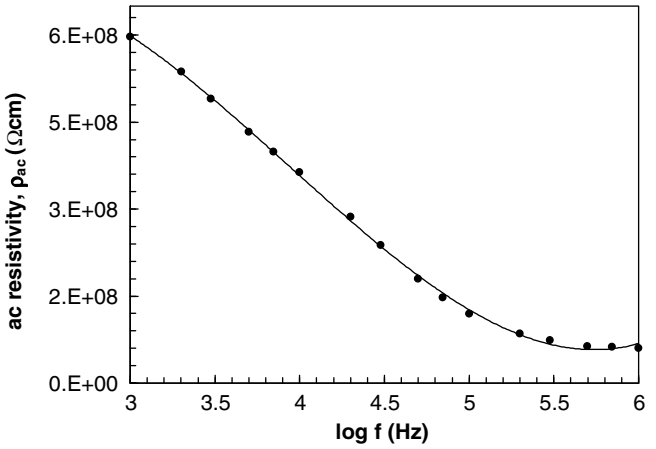

Fig. 4. Variation of ac resistivity (ρ_{ac}) with frequency.

In addition, Fig. 5 shows the dependence of resistivity of MIS structure on frequency at room temperature. It is seen that resistivity decreases as frequency increases. An ac field of sufficiently high frequency applied to a MIS structure, may cause a net polarization, which is out of phase with the field [46,47].

In this study the complex modulus plane analysis is based on the plot of the real part of M' versus the imaginary part of M'' over a wide range of frequencies. Fig. 6a and b are shown the M' and M'' of electric modulus M^* versus frequency for MIS structure at room temperature. As can be seen from the figures, as the frequency increases, M' and M'' increases to a maximum. Also M' and M'' increase as the frequency are increased and especially there are a sharp increase in the M' and M'' in the frequency range between 100 kHz and 1 MHz. Similar studies have been reported in literature [25–28,32,43,48].

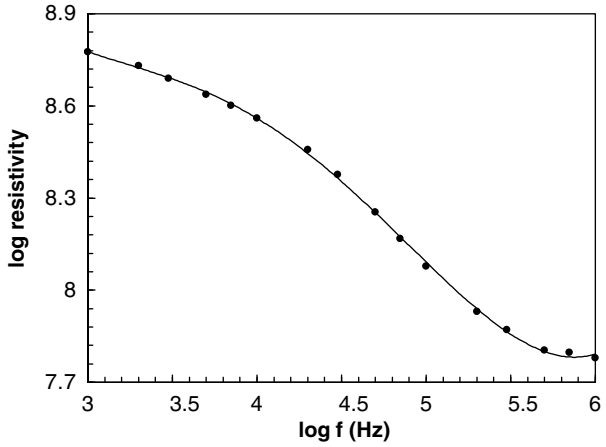

Fig. 5. Plot of log resistivity vs. log frequency for MIS structure at room temperature.

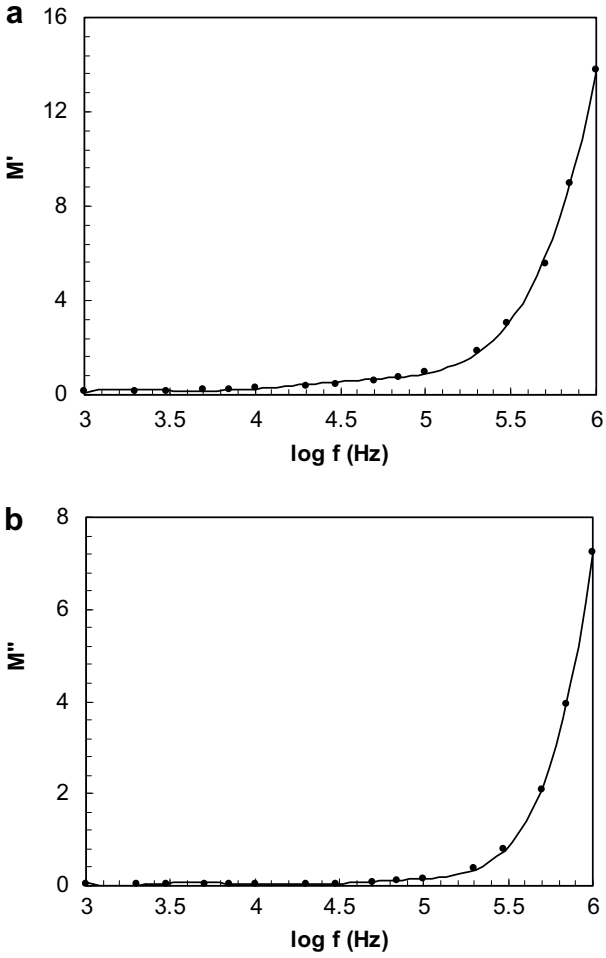

Fig. 6. (a) The real part M' and (b) the imaginary part M'' of electric modulus M^*, versus frequency, f, for MIS structure.

4. Conclusions

The electrical and dielectric properties of $Au/SnO_2/n$-Si (MIS) structure have been studied in detail in the wide frequency (1 kHz–1 MHz) range. The values of capacitance (C) and conductance (G/ω) decrease with increasing frequency. This observation may be attributed to the capacitive response of interface states to the measurement. The values of dielectric constant (ϵ') and dielectric loss (ϵ'') decrease with increasing frequency. These behaviors are attributed to the decrease of polarization with increasing frequency in the SnO_2/n-Si interface. Also, the ac electrical conductivity (σ_{ac}) increase with increasing frequency due to the accumulation of charge carries at the boundaries. As a result, the behavior of dielectric properties especially depends on frequency, interfacial insulator layer, the density of space charges and fixed surface charge.

Acknowledgments

This work is supported by Turkish of Prime Ministry State Planning Organization Project number 2001K120590, Gazi University Scientific Research Project (BAP) FEF. 05/2008-19 and FEF. 05/2008-23.

References

[1] V. Vasu, A. Subrahmanyan, Thin Solid Films 202 (1991) 283.
[2] N. Srinivasa Murty, S.R. Jawalekar, Thin Solid Films 108 (1983) 277.
[3] E. Elangovan, K. Ramamurthi, Cryst. Res. Technol. 38 (2003) 779.
[4] S. Munnix, M. Schmeits, Phys. Rev. B 27 (1983) 7624.
[5] W. Göpel, K.D. Schierbaum, Sens. Actuators B 26–27 (1995) 1.
[6] Ç. Kılıç, A. Zunger, Phys. Rev. Lett. 88 (2002) 095501.
[7] K.L. Chopra, S. Major, D.K. Pandya, Thin Solid Films 102 (1983) 1.
[8] J. Joseph, V. Mathew, K.E. Abraham, Cryst. Res. Technol. 41 (2006) 1020.
[9] E.H. Nicollian, J.R. Brews, Metal Oxide Semiconductor (MOS) Physics and Technology, Wiley, New York, 1982.
[10] S.M. Sze, Physics of Semiconductor Devices, 2nd ed., Willey, New York, 1981.
[11] C.R. Crowell, S.M. Sze, J. Appl. Phys. 36 (1965) 3212.
[12] Z. Quennoughı, Phys. Status Solidi (a) 160 (1997) 127.
[13] H.S. Haddara, M. El-Sayed, Solid State Electron. 31 (8) (1988) 1289.
[14] P. Cova, A. Singh, R.A. Masut, J. Appl. Phys. 82 (1997) 5217.
[15] E.H. Nicollian, A. Goetzberger, Appl. Phys. Lett. 7 (1965) 216.
[16] S. Kar, S. Varma, J. Appl. Phys. 58 (11) (1985) 4256.
[17] H. Deuling, E. Klausmann, A. Goetzberger, Solid State Electron. 15 (5) (1972) 559.
[18] R. Castagne, A. Vapaille, Surf. Sci. 28 (1) (1971) 157.
[19] M. Kuhn, Solid State Electron. 13 (6) (1970) 873.
[20] B. Akkal, Z. Benamara, B. Gruzza, L. Bideux, Vacuum 57 (2000) 219.
[21] P. Chattopadhyay, B. Raychaudhuri, Solid State Electron. 35 (1993) 605.
[22] Ş. Aydoğan, M. Sağlam, A. Türüt, Polymer 46 (2005) 10982.
[23] C.P. Symth, Dielectric Behaviour and Structure, McGraw-Hill, New York, 1955.
[24] Vera V. Daniel, Dielectric Relaxation, Academic Press, London, 1967.
[25] N.G. McCrum, B.E. Read, G. Williams, Anelastic and Dielectric Effects in Polymeric Solids, Wiley, New York, 1967.
[26] H. Wagner, R. Richert, Polymer 38 (1997) 5801.
[27] C. Leon, M.L. Lucia, J. Santamaria, Phys. Rev. B 55 (1998) 882.
[28] M.S. Mattsson, G.A. Niklasson, K. Forsgren, A. Harsta, J. Appl. Phys. 85 (4) (1999) 2185.
[29] M. Popescu, I. Bunget, Physics of Solid Dielectrics, Elsevier, Amsterdam, 1984.
[30] A. Chelkowski, Dielectric Physics, Elsevier, Amsterdam, 1980.
[31] A. Tataroğlu, Ş. Altındal, M.M. Bülbül, Microelectron. Eng. 81 (2005) 140.
[32] S.P. Szu, C.Y. Lin, Mater. Chem. Phys. 82 (2003) 295.
[33] D. Maurya, J. Kumar, Shripal, J. Phys. Chem. Solids 66 (2005) 1614.
[34] A.A. Sattar, S.A. Rahman, Phys. Status Solidi (a) 200 (2) (2003) 415.
[35] S.A. Nouh, S.A. Gaafar, H.M. Eissa, Phys. Status Solidi (a) 175 (1999) 699.
[36] A. Tataroğlu, Microelectron. Eng. 83 (2006) 2551.

[37] M.R. Ranga Raju, R.N.P. Choudhary, S. Ram, Phys. Status Solidi (b) 239 (2) (2003) 480.
[38] A.S.Md.S. Rahman, M.H. Islam, C.A. Hogarth, Int. J. Electron. 62 (2) (1987) 167.
[39] C.V. Kannan, S. Ganesamoorthy, C. Subramanian, P. Ramasamy, Phys. Status Solidi (a) 196 (2) (2003) 465.
[40] K.S. Moon, H.D. Choi, A.K. Lee, K.Y. Cho, H.G. Yoon, K.S. Suh, J. Appl. Polym. Sci. 77 (2000) 1294.
[41] Z. Jiwei, Y. Xi, W. Mingzhong, Z. Liangying, J. Phys. D: Appl. Phys. 34 (2001) 1413.
[42] M. Rapos, M. Ruzinsky, S. Luby, J. Cervenk, Thin Solid Films 36 (1976) 103.
[43] M.D. Migahed, M. Ishra, T. Fahmy, A. Barakat, J. Phys. Chem. Solids 65 (2004) 1121.
[44] A.S. Riad, M.T. Korayem, T.G. Abdel-Malik, Physica B 270 (1999) 140.
[45] S.C. Watawe, B.D. Sarwade, S.S. Bellad, B.D. Sutar, B.K. Chougule, J. Magn. Magn. Mater. 214 (2000) 55.
[46] B. Taraev, Physics of Dielectric Materials, Mir Publication, Moscow, 1975.
[47] A.K. Jonscher, Nature 267 (1977) 673.
[48] K. Prabakar, S.K. Narayandass, D. Mangalaraj, Mater. Sci. Eng. B 98 (3) (2003) 225.